The Origin, Structure, and Tracks of the Monsoon Onset Vortex - Integrating Theory and Predictability Studies using the UFS for early season impacts on the Monsoon

Shreyas Dhavale[1,2], Anantha Aiyyer[1] and Cristiana Stan[3]

(sdhavale@ucar.edu / sdhaval2@ncsu.edu)

PhD Candidate at the Department of Marine, Earth and Atmospheric Sciences, North Carolina State University

NOAA WPO and UCAR CPAESS WINGS Fellow

(NOAA Science Collaboration Program award #NA21OAR4310383)

[1] *Department of Marine, Earth and Atmospheric Sciences, North Carolina State University*

[2] *University Corporation for Atmospheric Research*

[3] *Department of Atmospheric, Oceanic and Earth Sciences, George Mason University, Fairfax, VA, USA*

Presentation Outline

1. Background and Introduction
2. Usefulness of this study
3. Data
4. Results
    a) Large-scale features of the Monsoon
    b) Case studies of the Monsoon Onset Vortex (2011, 2014 and 2015)
5. Summary

1. Introduction and Background

An overview of the Indian Summer Monsoon

- Extends from June to September
- Mascarene High
- Somali Jet (low level jet at 850 hPa)

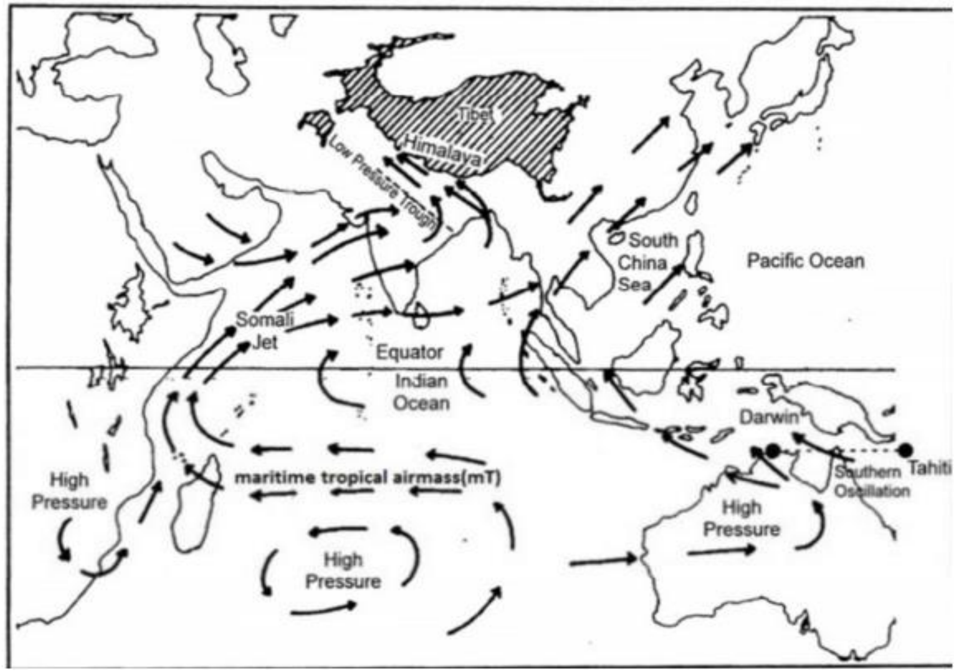

- Tropical easterly jet (TEJ)
- Tibetan High

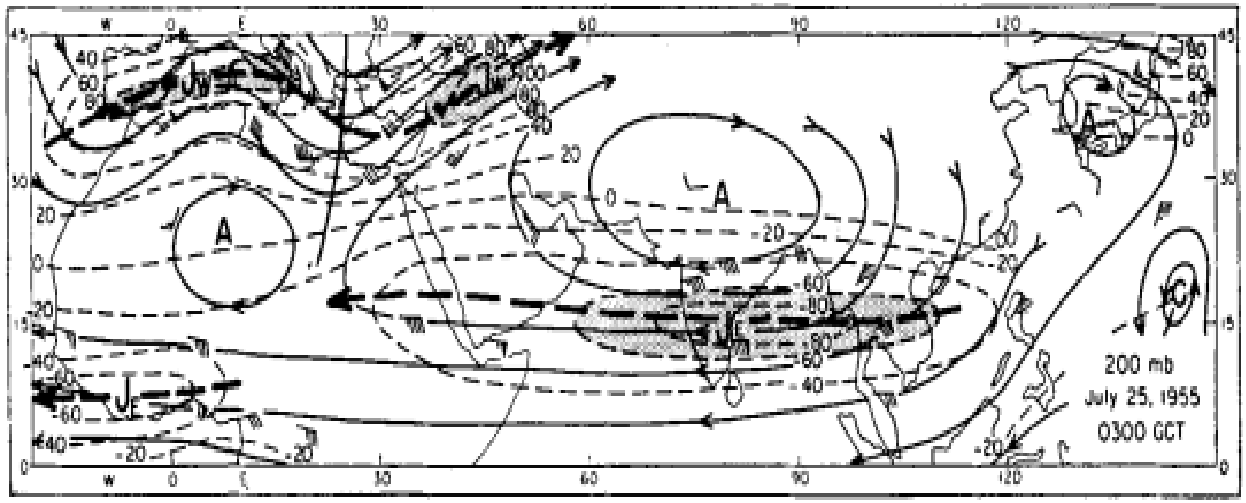

Fig. 4 c. Streamlines and isotachs 200 mbs, July 25, 1955. Jet axis marked heavy and wind maxima shaded.

Image from Koteswaram, P. (1958)

The Monsoon Onset Vortex

- During the Monsoon, there is high vertical wind shear over the Arabian Sea: low-level westerlies and upper-level easterlies

- Tropical cyclogenesis is rare during the core monsoon period of July-August

- However, during the Monsoon onset phase (**late May-early June**), a vortex forms in the Arabian Sea in ~60% of the years

- This vortex is termed as the Monsoon Onset Vortex (MOV) - **synoptic scale feature, part of the planetary scale monsoon circulation**

- Recent example: Cyclone Biparjoy in the Arabian Sea, June 2023

Cyclone Biparjoy - Infrared image from INSAT 3D during June 10, 2023

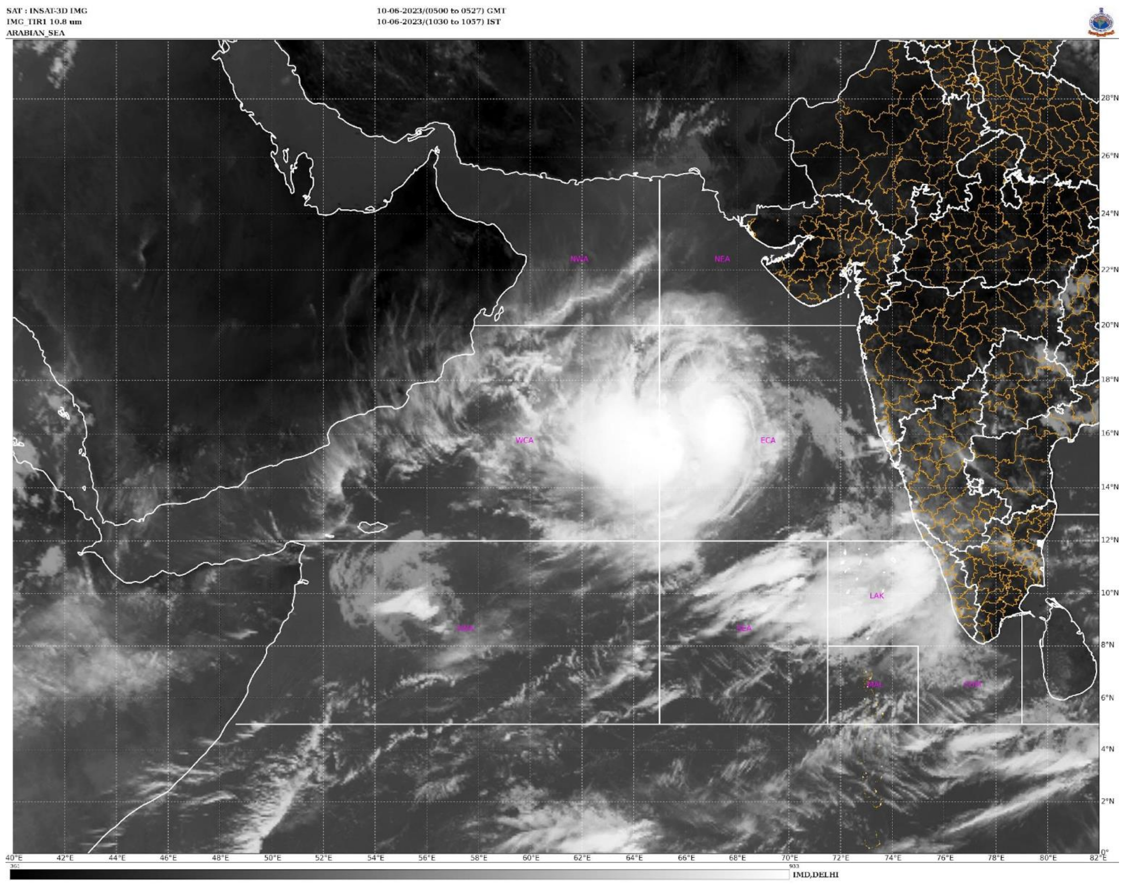

(Image credits: India Meteorological Department)

MOV in the context of the northward shift of monsoon precipitation

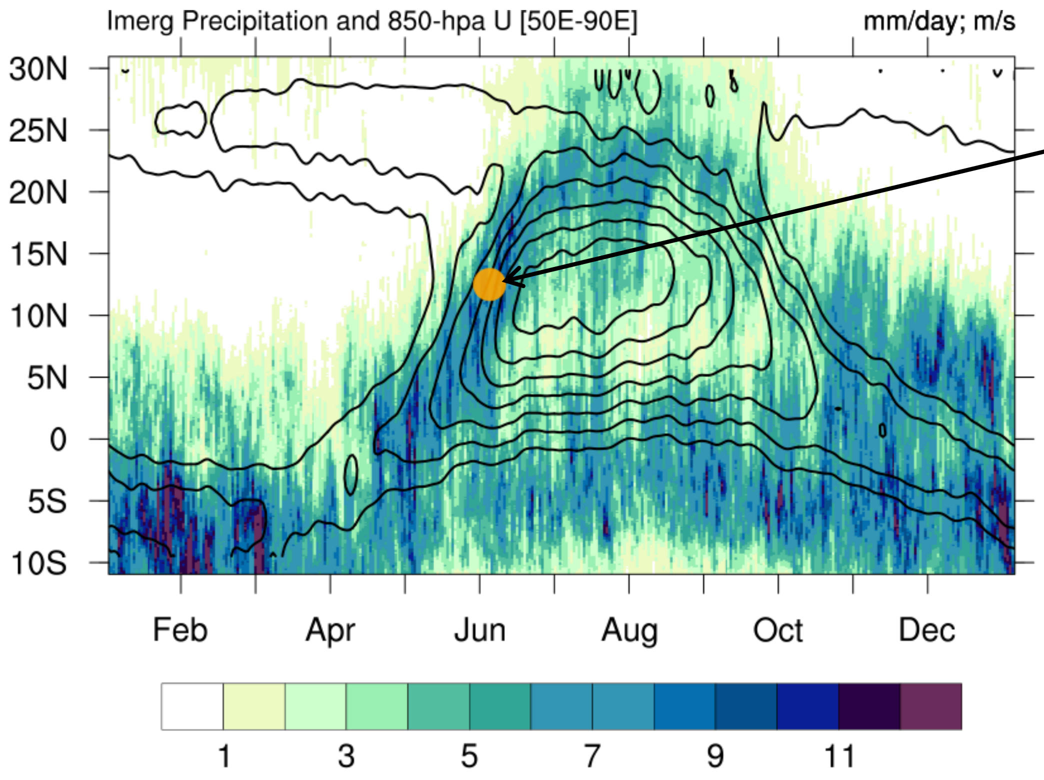

Figure: Latitude-time Hovmöller of climatological rainfall rate (shaded; mm day−1; NASA IMERG) and zonal wind (contours; ms−1; ERA-interim) averaged over 50E-80E longitudes. The median MOV genesis location (1980-2021) is marked by the orange dot.

MOV formation coincides with the rapid increase of zonal wind and the seasonal northward shift of precipitation.

2. Usefulness of this study

Impacts of the MOV

1. Affects the onset of the Monsoon
   - Can bring in the monsoon early or delay its advancement
   - MOVs becoming TCs can affect climatological wind pattern on a synoptic-subseasonal scale

2. Socio-Economic impacts
   - Most MOVs become TCs – destructive TCs in the past (e.g., 2007, 2010, Evan and Camargo, 2011)
   - Densely populated coastline
   - Marine trade routes

Previous studies

1. Barotropic instability of the Somali Jet (Krishnamurti et al., 1981).
2. Dry barotropic-baroclinic instability of basic state – idealized models with 2 or more atmospheric layers (e.g., Mak and Kao, 1982; Krishnakumar et al., 1993).
3. Synoptic studies on the environment of the MOV
   - Arabian Sea mini-warm pool: SSTs > 30.5°C (Rao and Sivakumar, 1999)
   - Somali jet and east-west shear zone (Deepa et. al., 2007).

- The mechanism governing MOV formation/growth is understudied.

- **No previous studies have focused on the predictability of the MOV and associated impacts on the early-season monsoon forecasts in short-medium range forecasts of global models.**

3. Data

Data

- **UFS S2S prototypes – P5, P6 and P8**
  - Grid spacing of 25 km
  - Reforecasts from April 2011 to March 2018.
  - Initialized on the 1st and 15th of each month, generates 35-day forecasts.

Validation Data:

- Atmosphere – ERA5 reanalysis
- MOV tracks – Joint Typhoon Warning Center (JTWC) Best track data
- Rainfall – GPM IMERG

4. Results

a) Large Scale Features of the Monsoon

Somali Jet Index and Monsoon rainfall

- Somali Jet Index – defined by Boos and Emanuel (2009).
- Given by the square root of twice the spatial mean kinetic energy of 850 hPa horizontal wind over the Arabian Sea (5°S-20°N, 50°E-70°E).

- **Strong 850 hPa winds over the Arabian Sea are linked with above normal rainfall over the west coast and central parts of India (Rajeevan et al., 2010).**

- How well do the UFS S2S prototypes capture this feature?

Somali Jet Index and Monsoon rainfall relation: June 15-July 19

P5

Anomalous rainfall (mm/day) for 1 std. dev. of jet index in P5

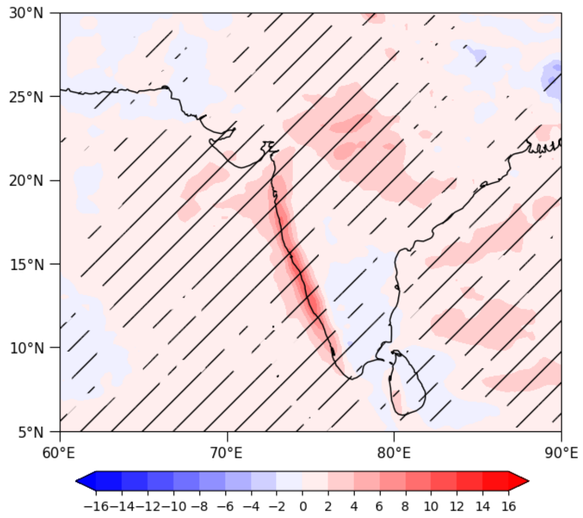

P6

Anomalous rainfall (mm/day) for 1 std. dev. of jet index in P6

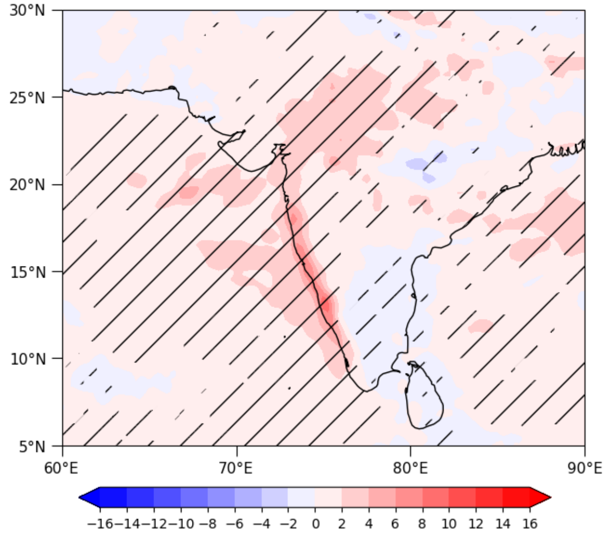

P8

Anomalous rainfall (mm/day) for 1 std. dev. of jet index in P8

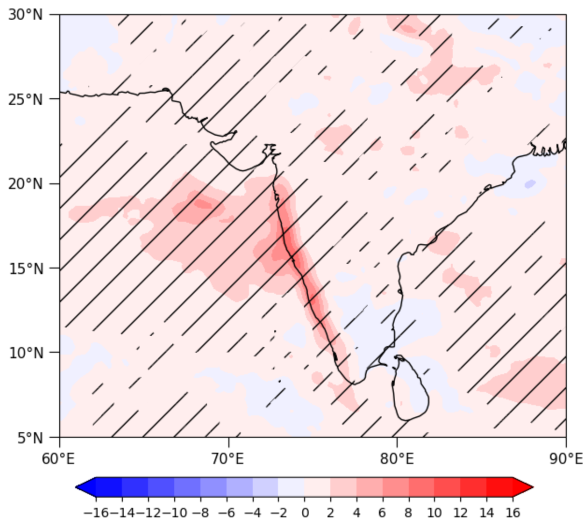

ERA5 & GPM

Anomalous rainfall for 1 std. dev. of jet index in ERA5

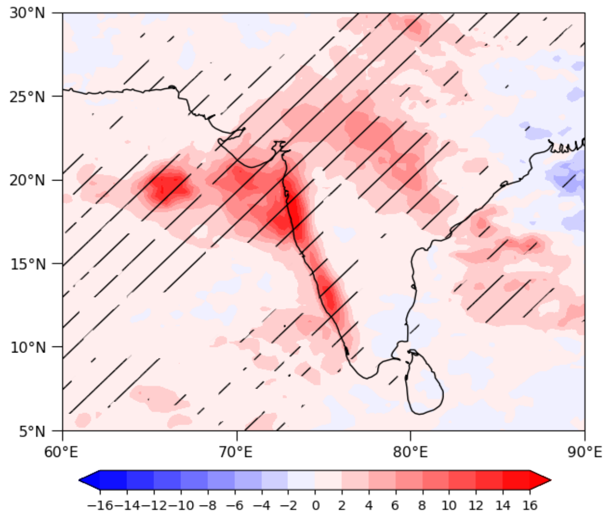

UFS run initialized on June 15 (early-season, but without MOV impacts)
The scaled slope term from the linear regression analysis between the total precipitation and Somali Jet Index from June 15 – July 19 during 2011-2017 → **anomalous rainfall in mm/day**

Areas marked by black lines are statistically significant at 95% confidence level.

UFS P5, P6 and P8 capture the spatial pattern of this relationship well, but underestimates the rainfall amount

4. Results

b) Case Studies of the MOV (2011, 2014 and 2015)

- MOV tracks, PV and diabatic heating profiles
- Precipitation
- Somali Jet Index

(UFS runs initialized on June 1)

MOV Diabatic heating and PV profiles

- Identify MOV center based on relative vorticity maxima at 850 hPa.
- Calculate the diabatic heating ($Q=d\theta/dt$, where θ is the potential temperature)
- Average the diabatic heating and PV from t-12 hours to t+12 hours and 2 degrees in latitude and longitude from the MOV center
- Compare the vertical profiles of the diabatic heating and PV between the UFS and ERA5

2015 MOV

- **Observations:** Forms on 06 UTC on June 6 from the vertical alignment of 2 vortices – a lead time of ~ 5 days for the UFS. Becomes a TC. Convectively active MJO in phase 2.
- **P5:** Forms on the same day as observations (~00 UTC on June 6), seems to form mainly from a top-down development. Becomes a TC.
- **P6:** Forms on the same day as observations (~00 UTC on June 6), forms from the vertical alignment of 2 vortices. Becomes a TC.
- **P8:** Forms on the same day as observations (~06 UTC on June 6), the vertical alignment of the 2 vortices is most clearly visible. Becomes a TC.
- Cold core vortex in all cases.

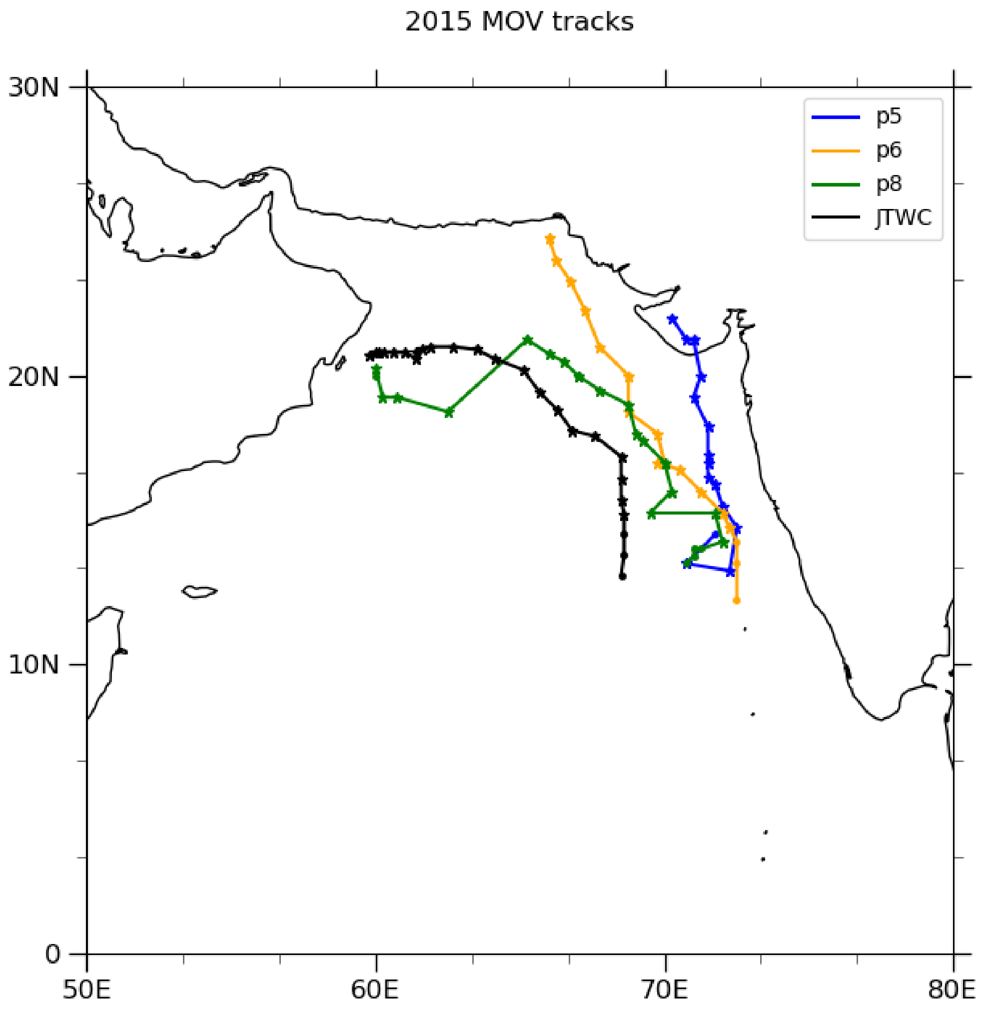

Somali Jet Index in 2015

- Somali Jet Index is predicted well in the UFS 2015
- MOV is captured well in 2015 and its track is forecasted close to observations in P8 – Somali Jet Index in P8 matches well with ERA5 even after the MOV formation (June 6).
- 2015 MOV influenced by MJO (phase 2)
- Better MJO predictions in P8 (Stefanova et al. 2022)

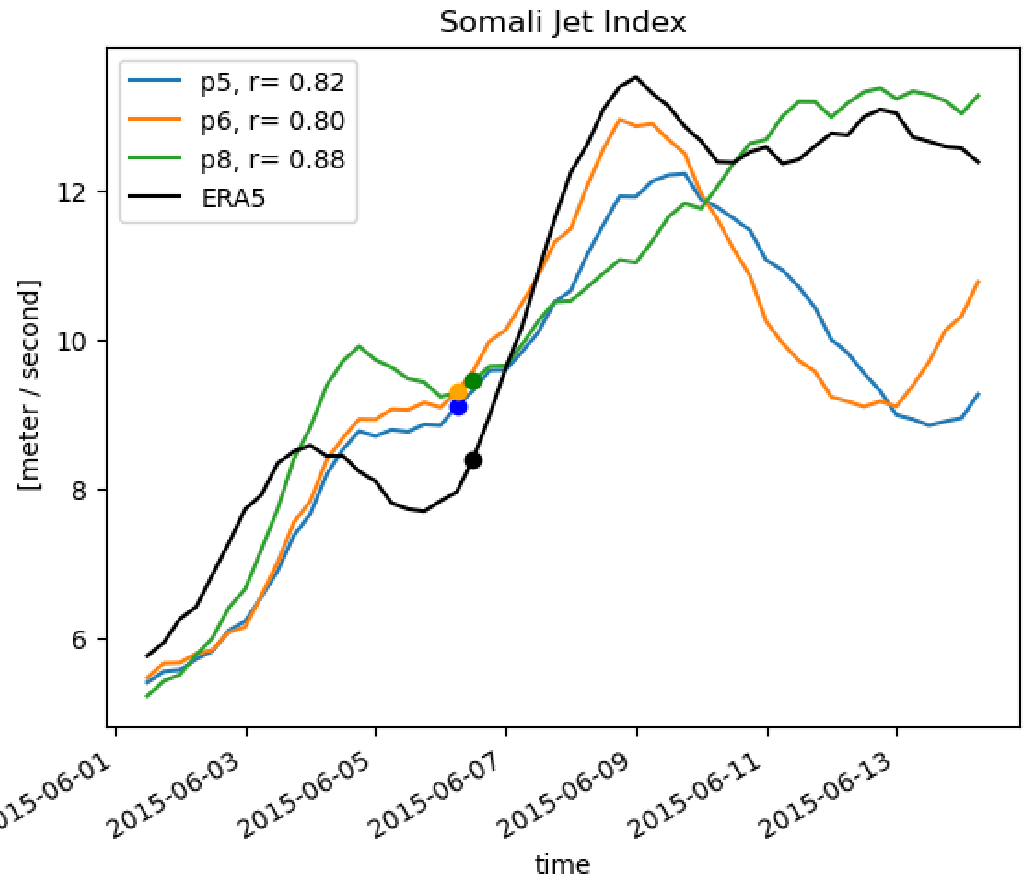

Somali jet index values smoothed over a 5-day period.

Rainfall difference from June 1-14, 2015

P5

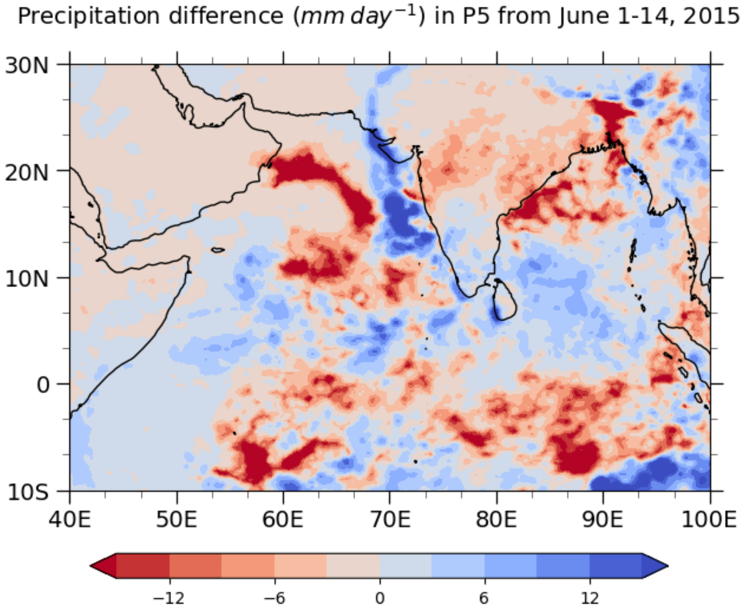

P6

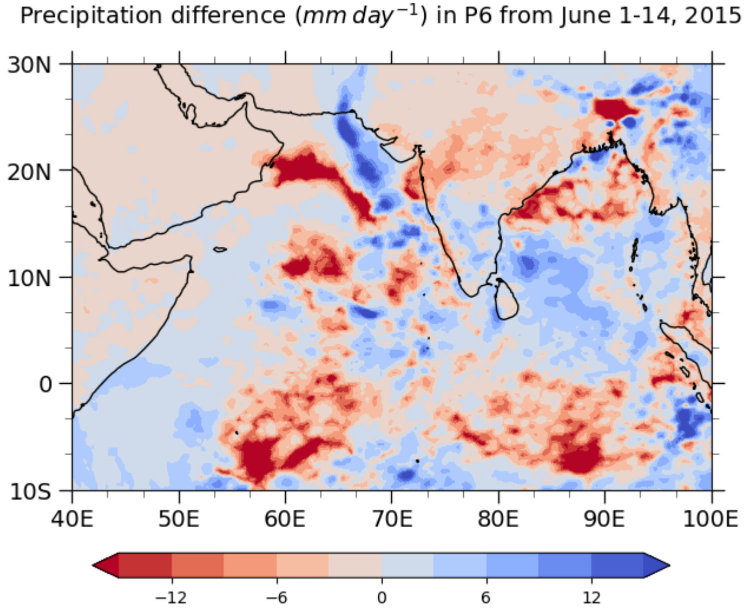

P8

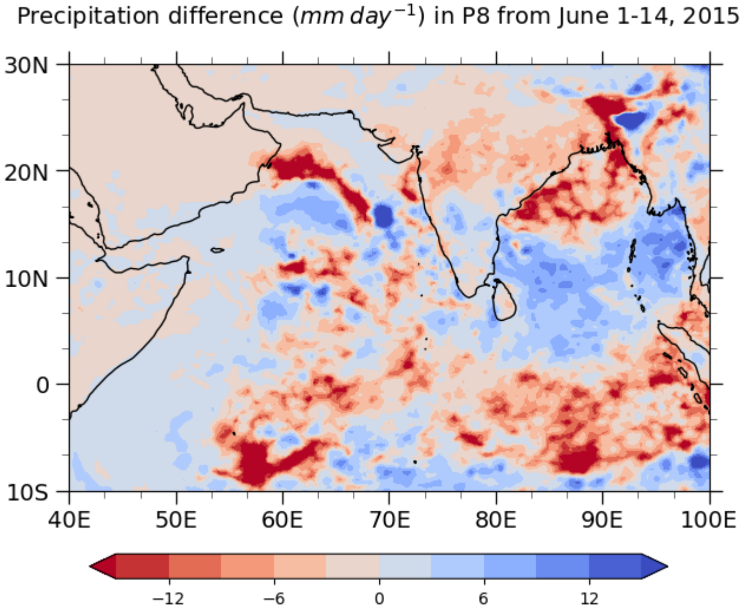

- Rainfall bias is the least in P8 followed by P6 and P5.
- High precipitation is seen along the MOV track.

- UFS does not capture heavy rainfall regions in the southern Indian Ocean, the Bay of Bengal and the northeastern parts of India.

PV

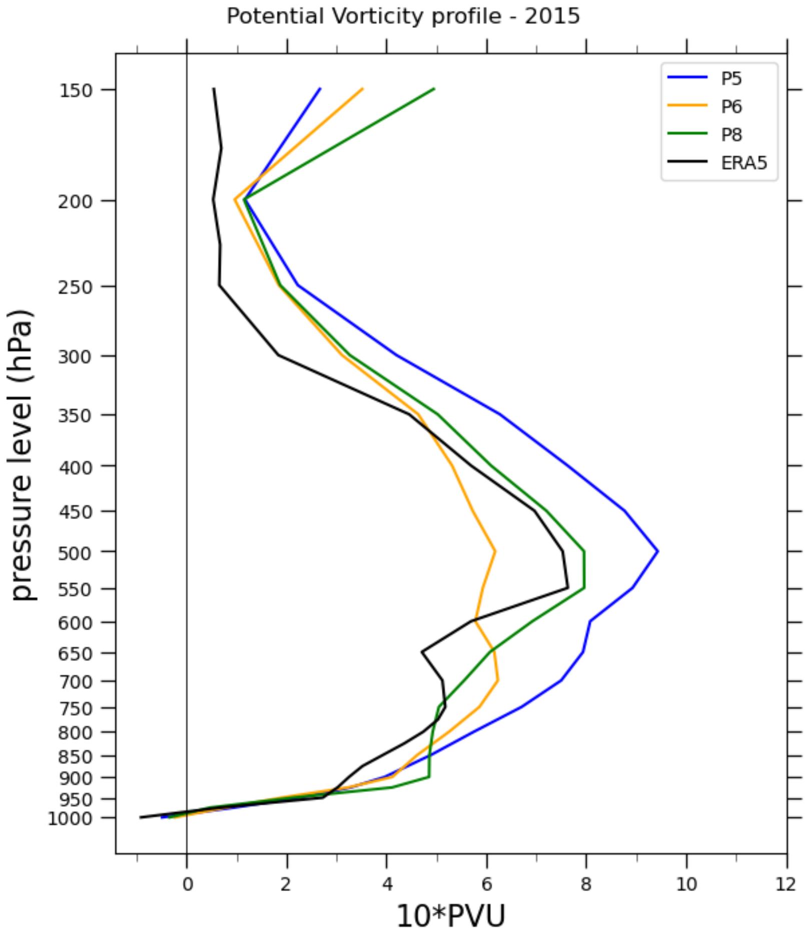

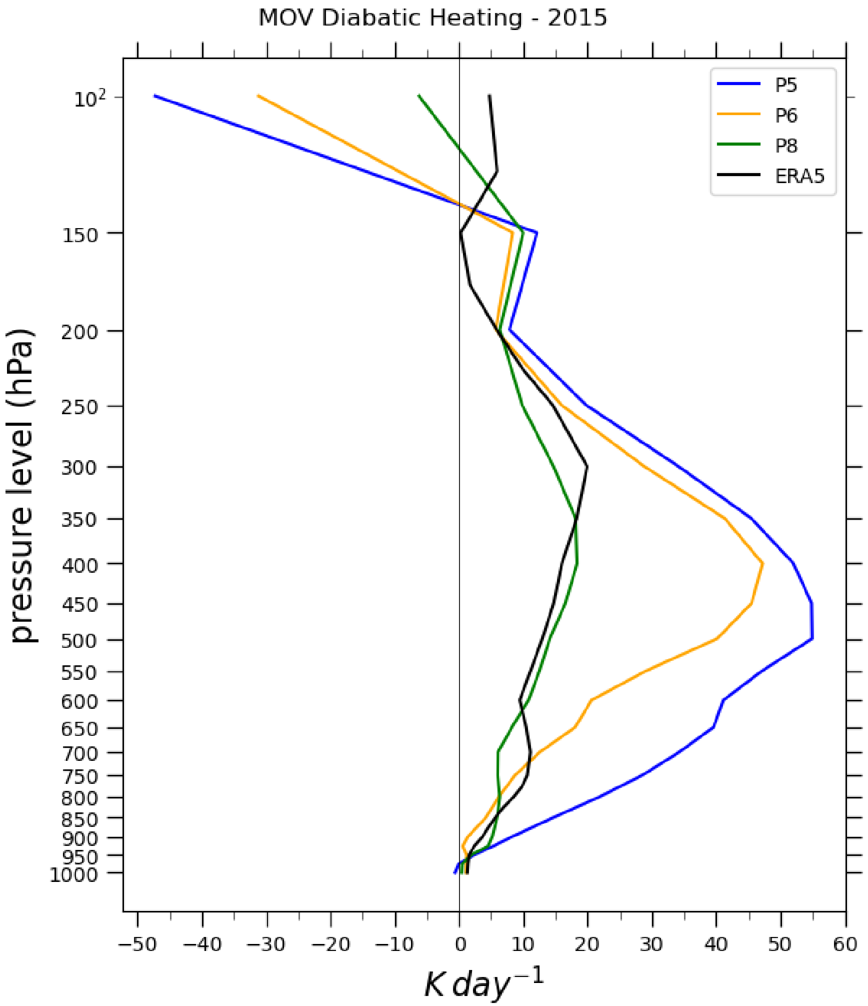

Diabatic Heating

Diabatic cooling in UFS above 150 hPa

- PV maxima in UFS is located slightly higher than that in ERA5.
- PV and diabatic heating profiles in P8 match closely with ERA5 – P8 had the best forecast of 2015 MOV
  - Accurate forecast of diabatic processes → higher forecast accuracy?
- High diabatic heating in P6, but PV magnitude is lower

2014 MOV

- **Observations:** Forms on 06 UTC on June 8 from the vertical alignment of 2 vortices – a lead time of ~7 days for the UFS. Becomes a TC.
- **P5:** Forms on the same day as observations (~06 UTC on June 8), forms from the vertical alignment of the 2 vortices but is weak in intensity (not a TC).
- **P6:** Forms ~1.5 days earlier (~18 UTC on June 6) but to the southeast of the observed location, forms from the vertical alignment of the 2 vortices. Becomes a TC.
- **P8:** No MOV forms at a lead time of 7 days. Mid-level vortex exists, but the cyclonic wind circulation does not extend down to the surface.
- Cold core vortex in all cases.

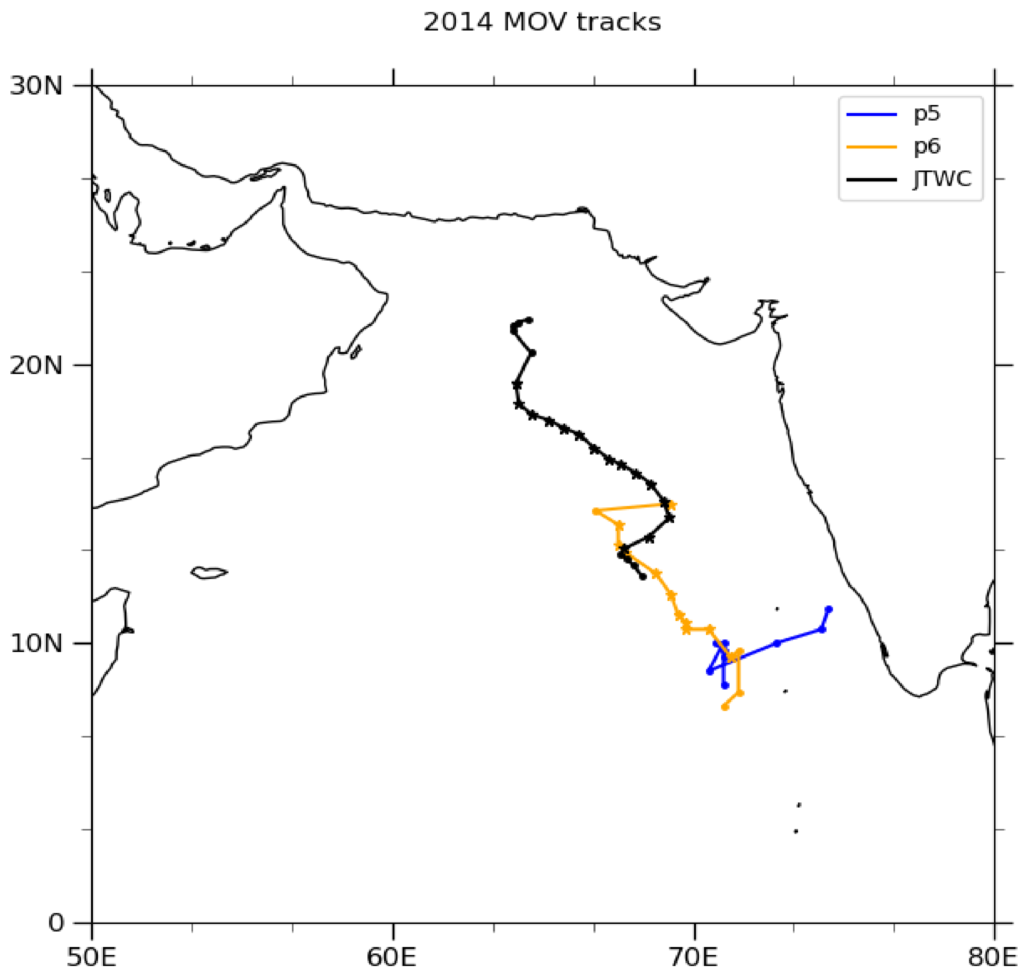

Somali Jet Index in 2014

- Somali Jet Index is well predicted by the UFS.
- The correlation and magnitude is slightly better in P6 and P8 even after June 9.
- MOV track was different in P5 (magnitude of the Jet Index differs after MOV formation)
- No MOV formed in P8, but jet index is captured well – need to resolve convection better?

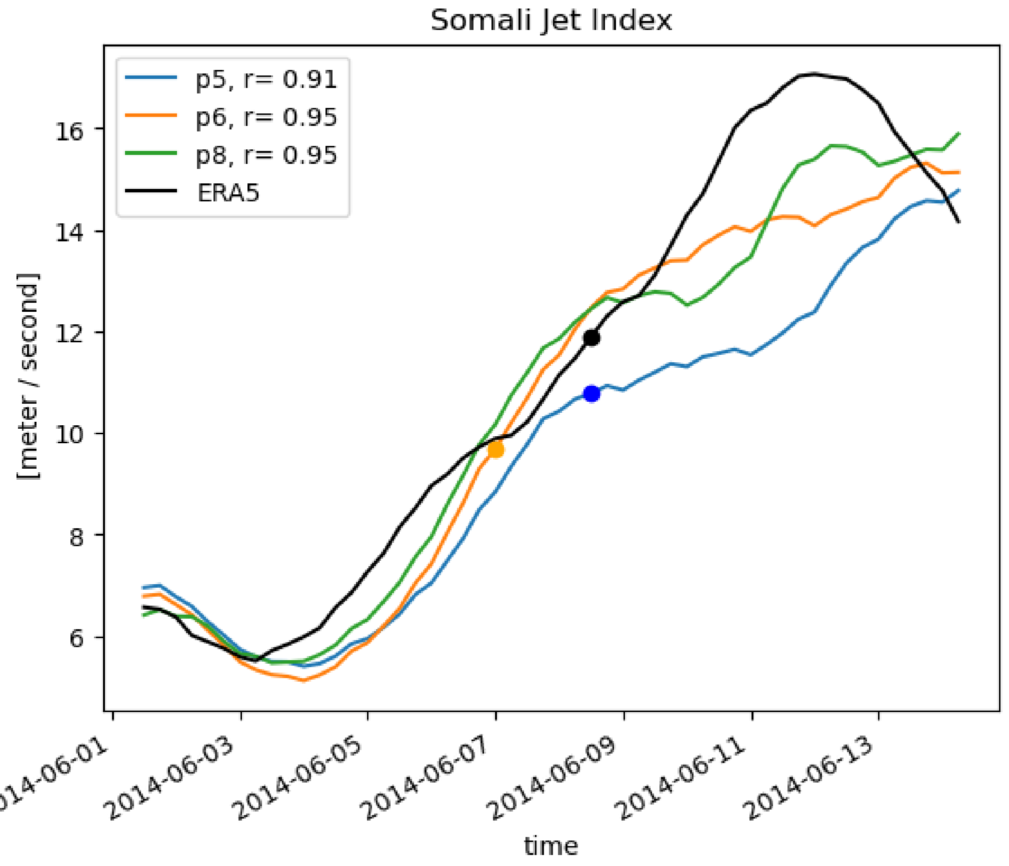

Somali jet index values smoothed over a 5-day period.

Rainfall difference from June 1-14, 2014

P5

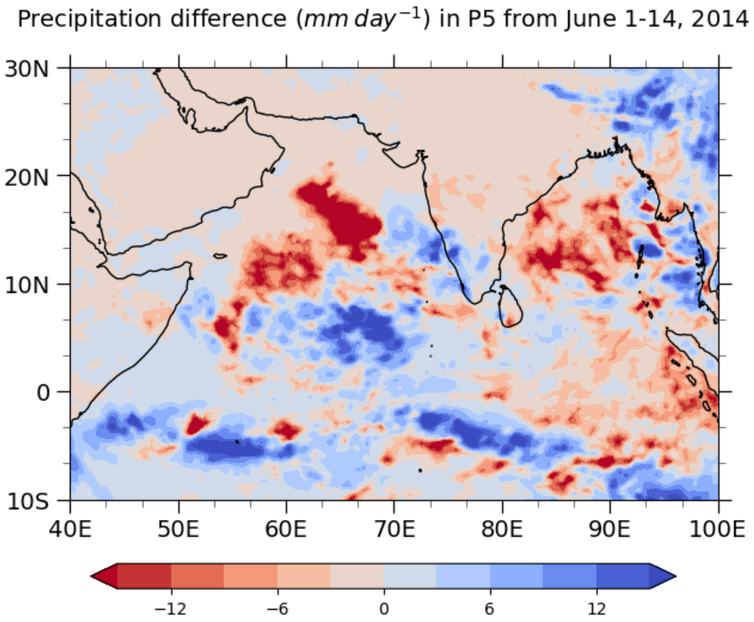

P6

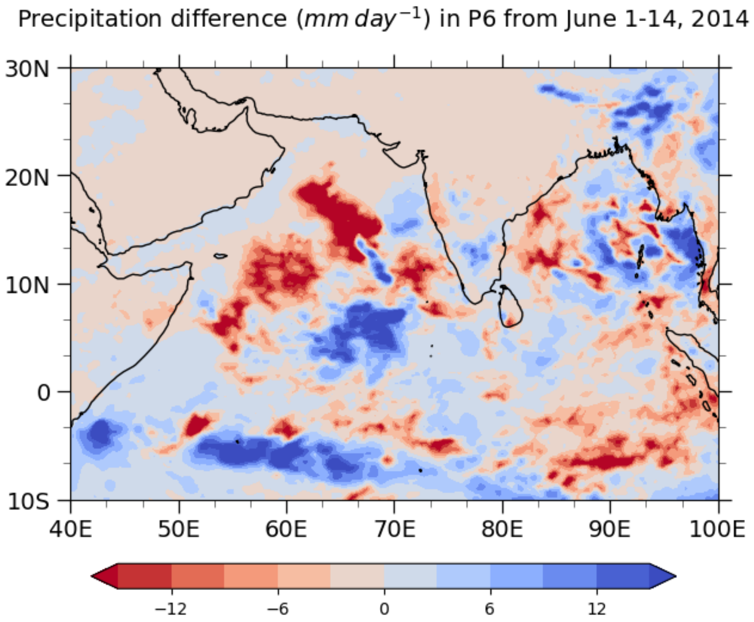

P8

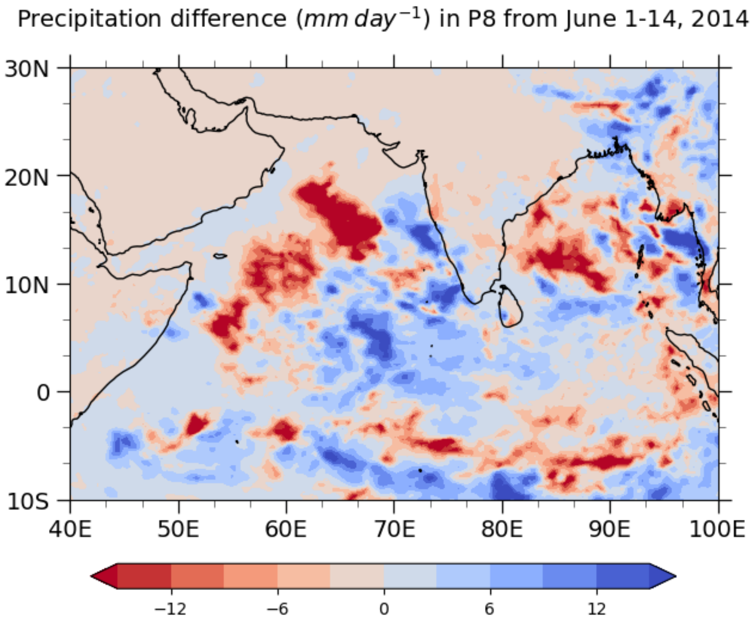

- Wet bias for southern parts of the west coast of India in P5 due to the MOV track
- Rainfall bias for the west coast is less in P6 followed by P8.

PV

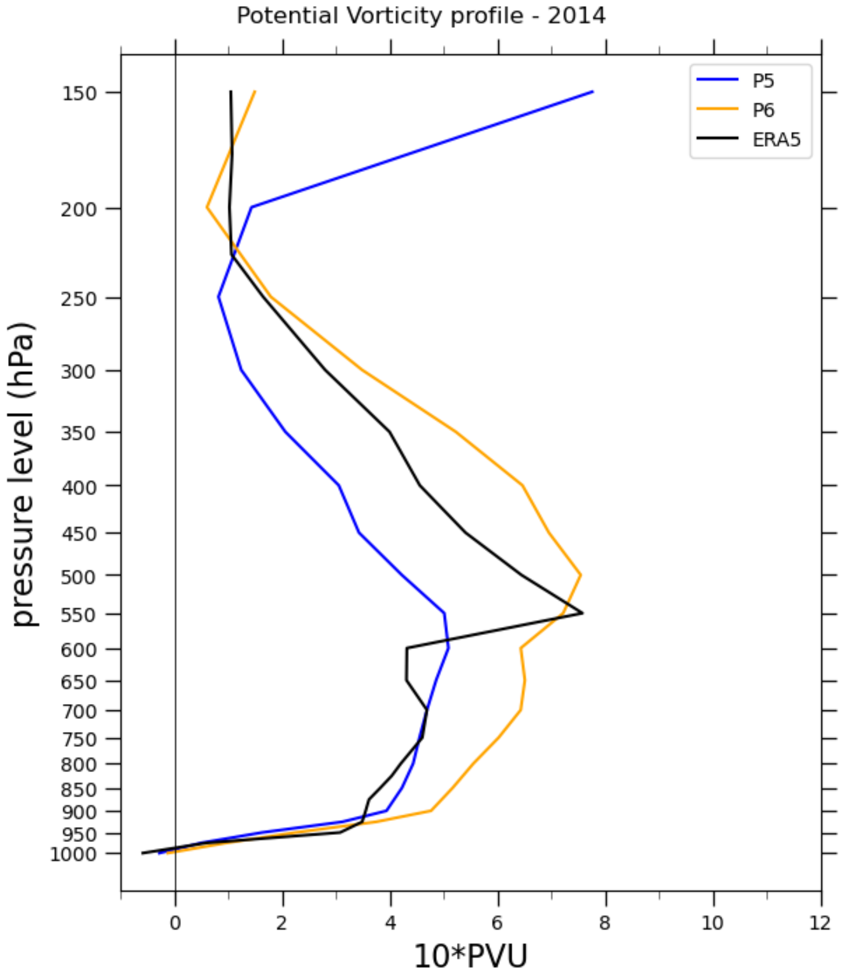

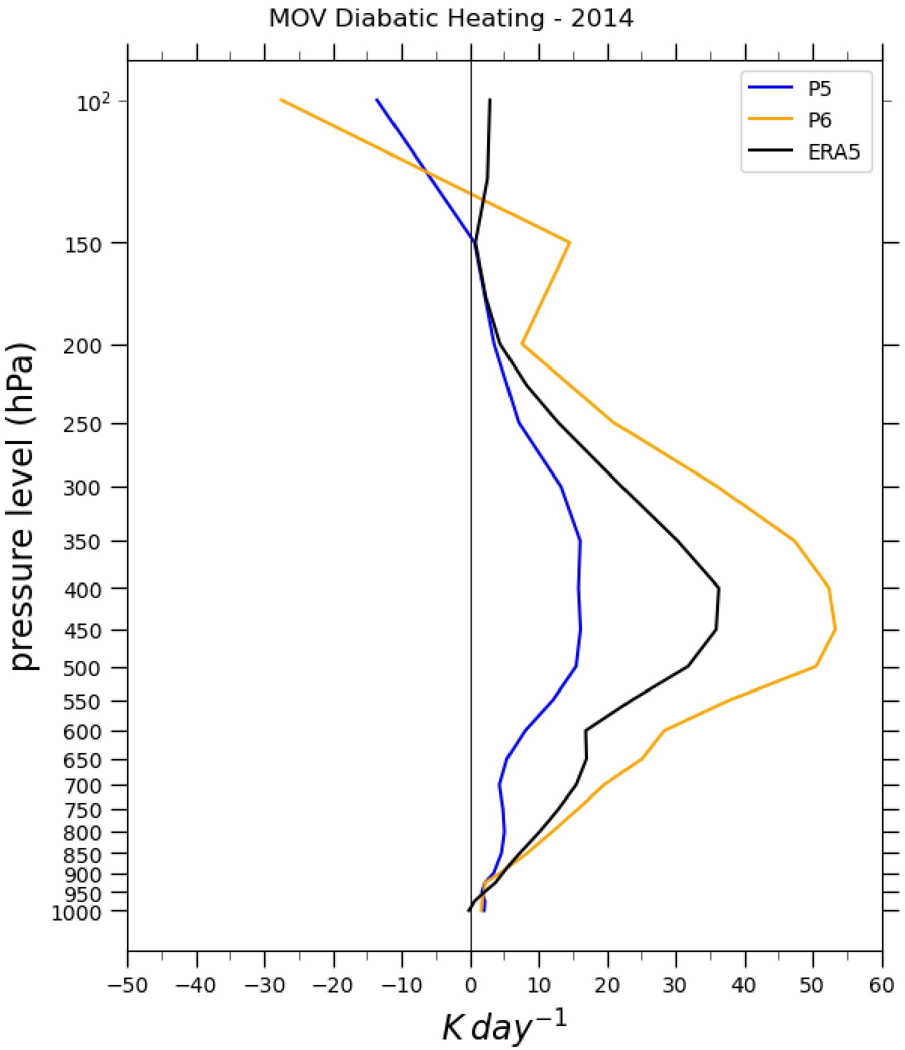

Diabatic Heating

Diabatic cooling in UFS above 150 hPa

- 2 PV maxima in ERA5, somewhat captured in P6.
- PV maxima in P6 is slightly higher than that in P5.
- Weak MOV in P5, less PV and less diabatic heating compared to ERA5.
- High diabatic heating in P6, overall PV is higher in P6, but max PV is not significantly higher than ERA5.

2011 MOV

- **Observations:** Forms on 06 UTC on June 9 from the vertical alignment of 2 vortices – a lead time of ~8 days for the UFS. Becomes a TC
- **P5:** Forms by ~18 UTC of June 3, around 5.5 days prior to observations. Does not form by the vertical alignment of two vortices. Becomes a TC
- **P6:** Forms ~ 00UTC of June 5, around 4 days prior to observations. Forms by the vertical alignment of two vortices. Becomes a TC
- **P8:** Forms by ~00 UTC of June 4, around 5 days prior to observations. Does not form by the vertical alignment of two vortices. No TC.
- Cold core vortex in all cases.

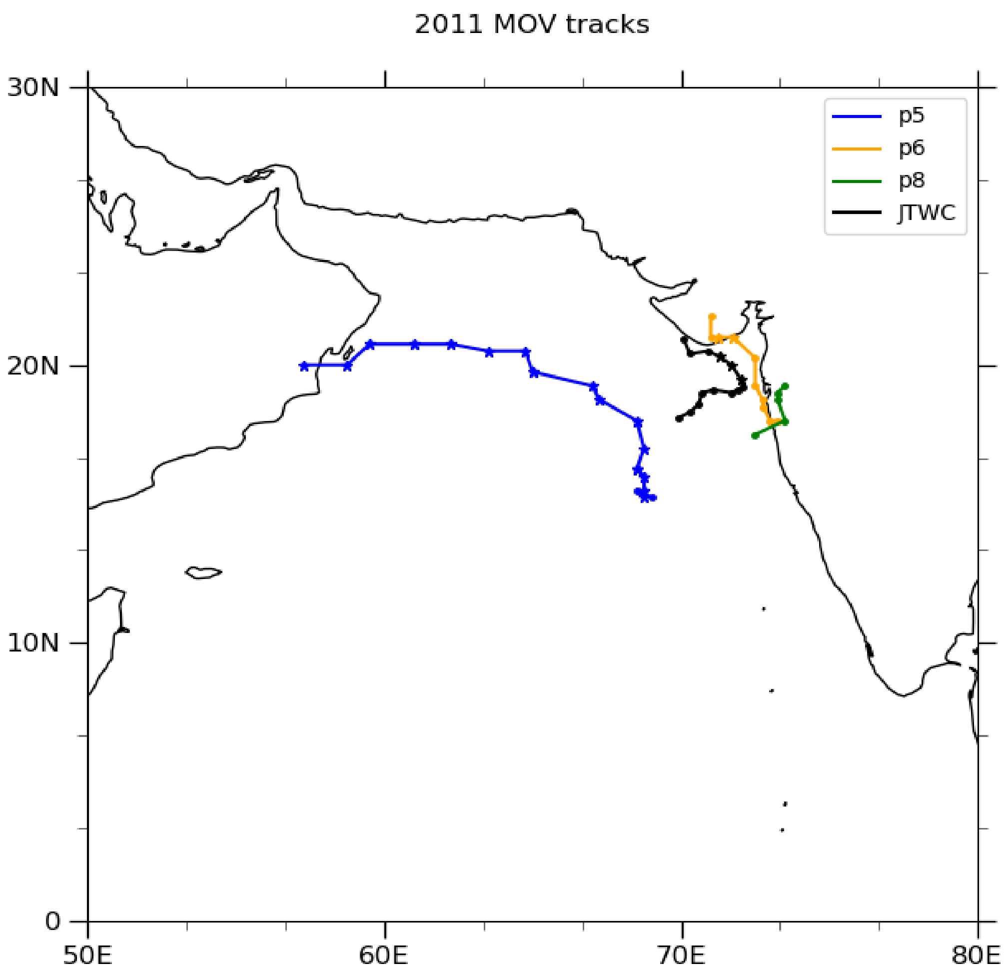

Somali Jet Index in 2011

- Considerable difference in the magnitude from June 2/3.
- MOV is not well captured by the UFS in 2011 (specifically P5).
- Somali Jet index in UFS differs from ERA5 even after the MOV has formed in the UFS
- Differences in OLR/precipitation in the UFS and observations on June 1 – role of initial conditions?

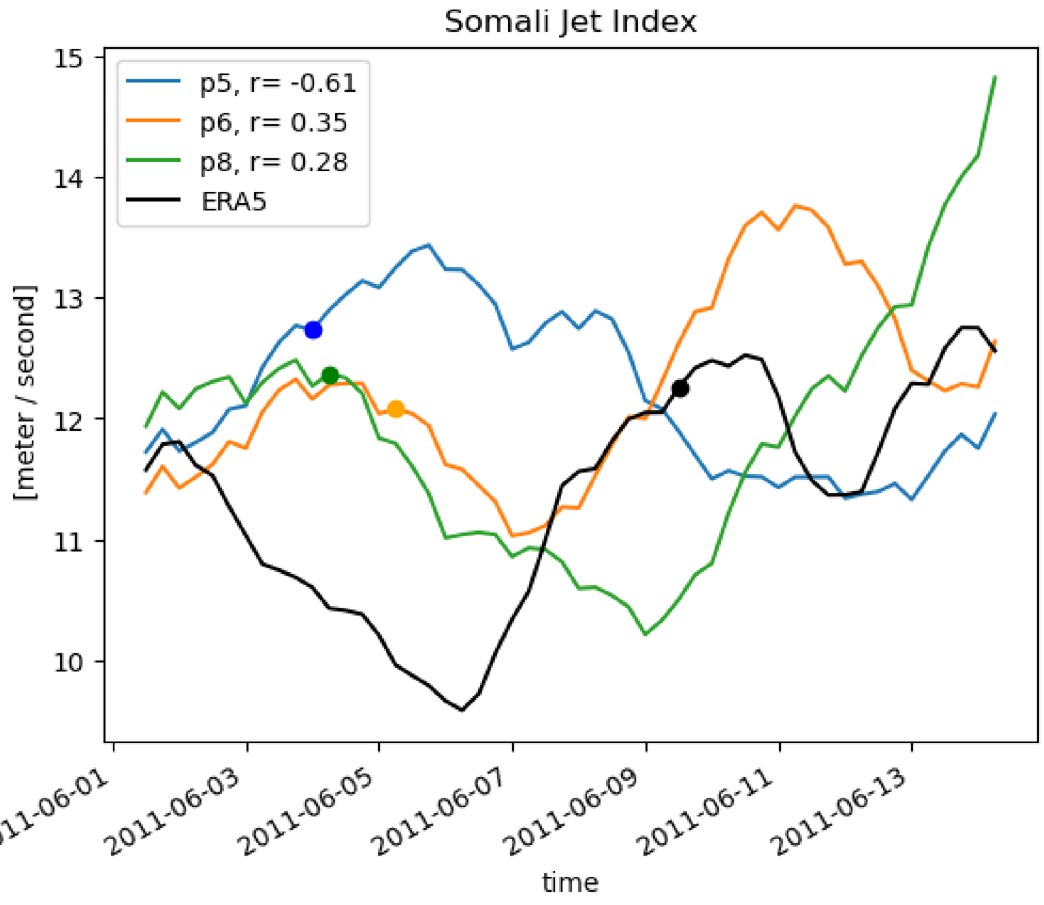

Somali jet index values smoothed over a 5-day period.

Rainfall difference from June 1-14, 2011

P5

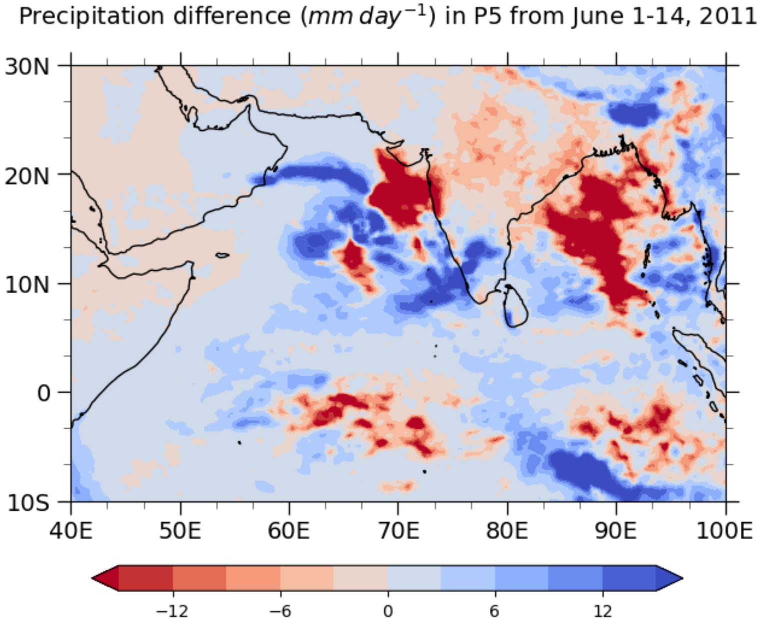

P6

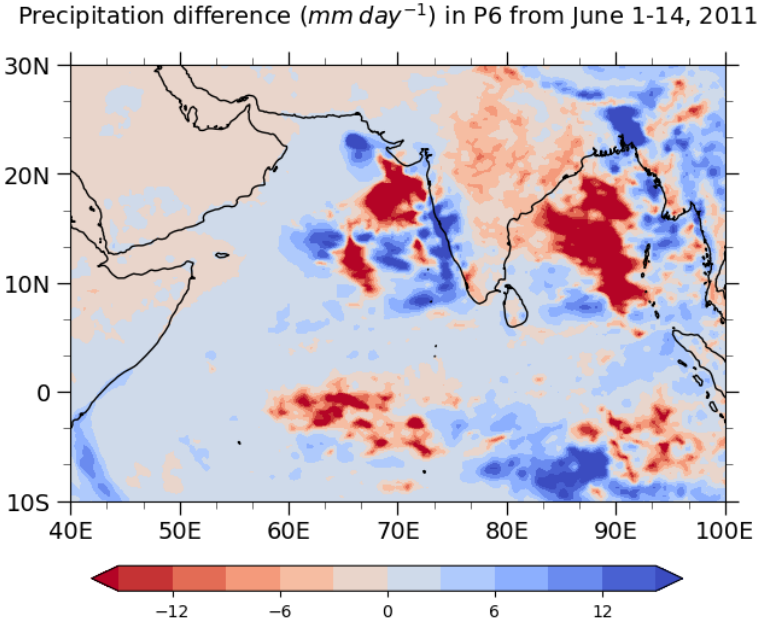

P8

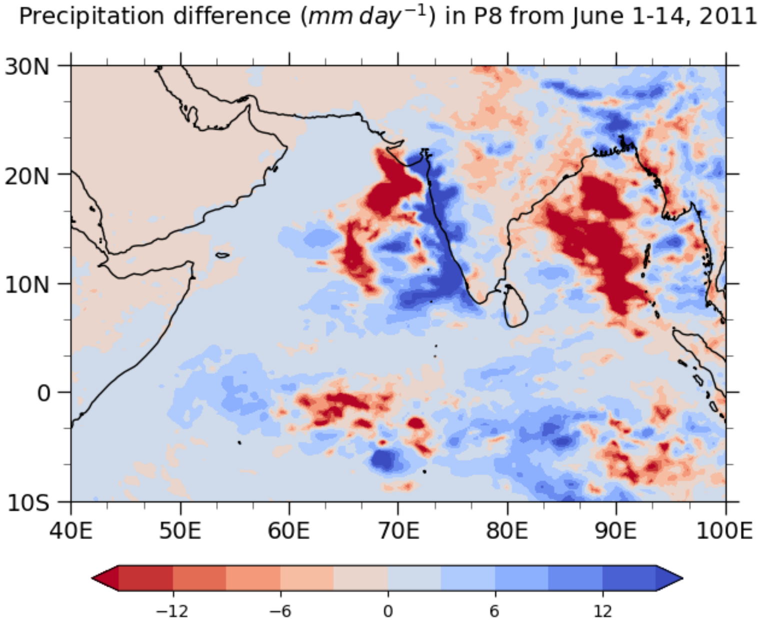

- MOV track influences rainfall variability to a large extent – heavy rainfall is seen along the MOV track.
- UFS forecast for the 2011 MOV track differs from observations → large rainfall bias in the first 2 weeks from initialization

PV

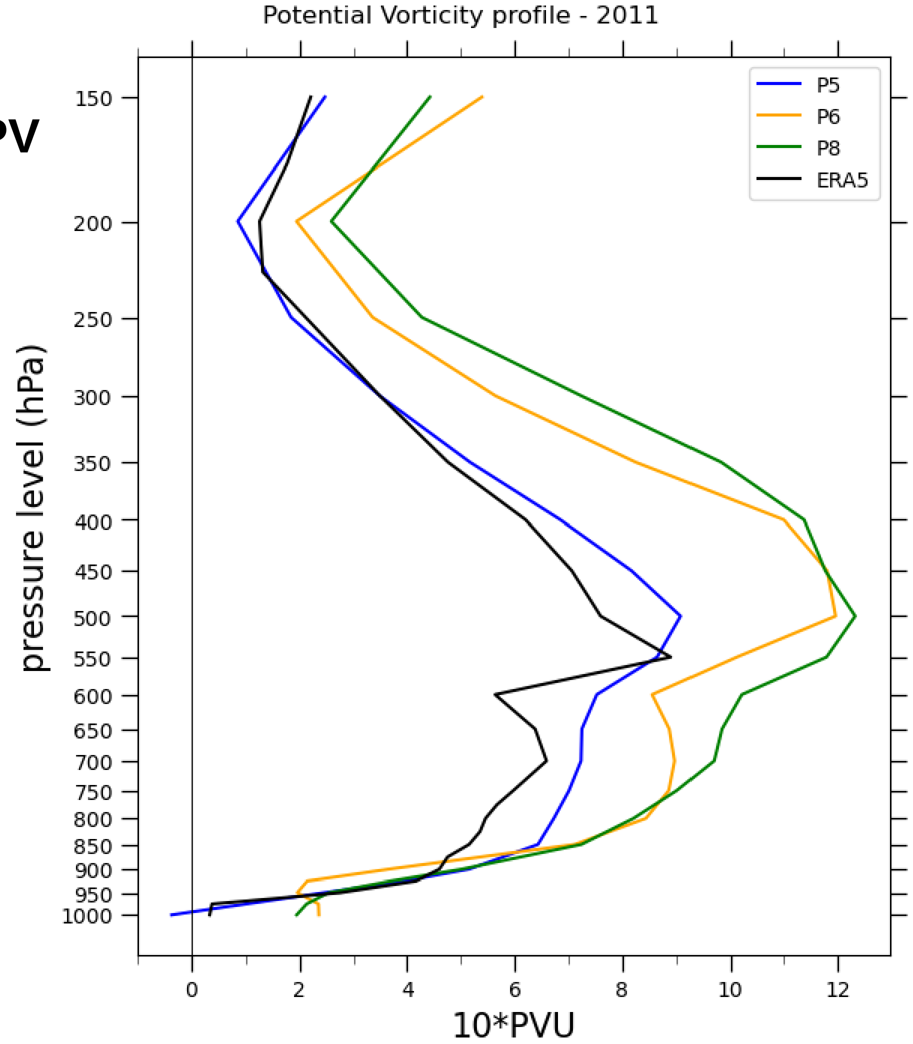

Diabatic Heating

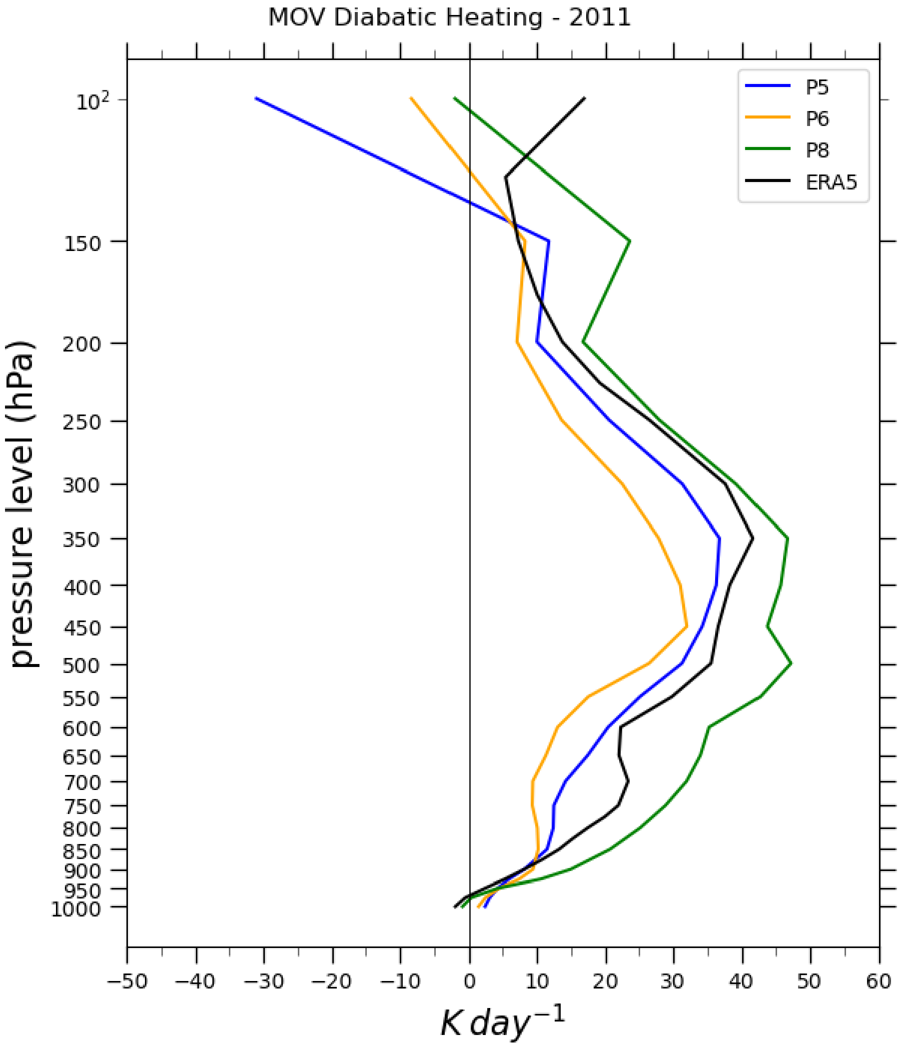

Diabatic cooling in UFS above 150 hPa

- PV maxima in UFS (~500 hPa) is higher than ERA5 (~550 hPa).
- PV profile of P5 matches with ERA5 below 900 hPa and above 400 hPa, however 2 distinct PV maxima are not well captured.
- Diabatic heating magnitude doesn’t match with PV amplitude – e.g. high PV in P5 and P6 is likely not due to diabatic heating.
- Peak Diabatic heating in P6 is lower than ERA5.

5. Summary

Key Takeaways

- The Somali Jet Index is a useful metric for studying early-season Monsoon rainfall variability
  - Stronger Somali Jet leads to heavier rain for west coast and central parts of India
  - UFS captures this relationship well

- The Somali Jet index is predicted well in 2014 and 2015, but no MOV in 2014 in P8
  - Mesoscale convective processes important and need to be captured well for MOV formation and prediction
  - Findings similar to conclusions from Dhavale and Aiyyer, 2024 – diabatic processes are the main factors for MOV formation

- All 3 prototypes forecast 2015 MOV, with the P8 forecast matching well with the observations
  - PV and diabatic effects are forecasted well for P8 → important for MOV forecasting

- The 2011 MOV was not well forecasted – differences in initial conditions?
- Overall, P6 and P8 perform better than P5 for the 3 MOV cases
- These 3 MOVs are not predicted by the UFS in the runs initialized on May 15th

Usefulness for S2S prediction

- MOV – extreme event in the context of monsoon onset and early season monsoon rainfall
- Highlights the importance of capturing mesoscale convective features for accurate subseasonal forecasts – this rationale can be applicable to tropical cyclones worldwide

- Somali Jet index – important parameter influencing S2S variability (850 hPa winds also incorporated in BSISO index calculation)
- Better forecasts for tropics/monsoons → better forecasts for midlatitudes through teleconnections (e.g., Beverly et al., 2021)

References

1. Beverley, J. D., Woolnough, S. J., Baker, L. H., Johnson, S. J., Weisheimer, A., & O'Reilly, C. H. (2021). Dynamical mechanisms linking Indian monsoon precipitation and the circumglobal teleconnection. Climate Dynamics, 57(9), 2615-2636.
2. Boos, W. R., & Emanuel, K. A. (2009). Annual intensification of the Somali jet in a quasi-equilibrium framework: Observational composites. *Quarterly Journal of the Royal Meteorological Society: A journal of the atmospheric sciences, applied meteorology and physical oceanography*, *135*(639), 319-335.
3. Deepa, R., Seetaramayya, P., Nagar, S. G., & Gnanaseelan, C. (2007). On the plausible reasons for the formation of onset vortex in the presence of Arabian Sea mini warm pool. Current Science, 794-800.
4. Dhavale, S., and Aiyyer, A. (2024). The Structure of a Developing Arabian Sea Monsoon Onset Vortex: Role of Moist Convection. Journal of Atmospheric Sciences (under review).
5. Evan AT, Camargo SJ. 2011. A climatology of Arabian Sea cyclonic storms. Journal of Climate, 24(1): 140–158. https://doi.org/10.1175/2010JCLI3611.1.
6. Halpern, D., & Woiceshyn, P. M. (2001). Somali jet in the Arabian Sea, El Niño, and India rainfall. Journal of Climate, 14(3), 434-441
7. Krishnamurti, T. N., P. Ardanuy, Y. Ramanathan, and R. Pasch, 1981: On the Onset Vortex of the Summer Monsoon. Monthly Weather Review, 109 (2), 344.
8. Krishnakumar, V., VS, K., & NR, K. (1993). Linear and non-linear studies of the summer monsoon onset vortex. Journal of the Meteorological Society of Japan. Ser. II, 71(1), 1-20.
9. Koteswaram, P. (1958). The easterly jet stream in the tropics. Tellus, 10(1), 43-57.
10. Mak, M., & KAO, C. Y. J. (1982). An instability study of the onset-vortex of the southwest monsoon, 1979. Tellus, 34(4), 358-368.
11. Rajeevan, M., Gadgil, S., & Bhate, J. (2010). Active and break spells of the Indian summer monsoon. Journal of earth system science, 119, 229-247.
12. Stefanova, L., Meixner, J., Wang, J., Ray, S., Mehra, A., Barlage, M., ... & Zheng, W. (2022). Description and results from UFS coupled prototypes for future global, ensemble and seasonal forecasts at NCEP.

Supplementary Slides

Comparison of Precipitation on June 1 for 2011 MOV

Total Precipitation: Initialized 2011-06-01T00 UTC, valid for 2011-06-01

P5

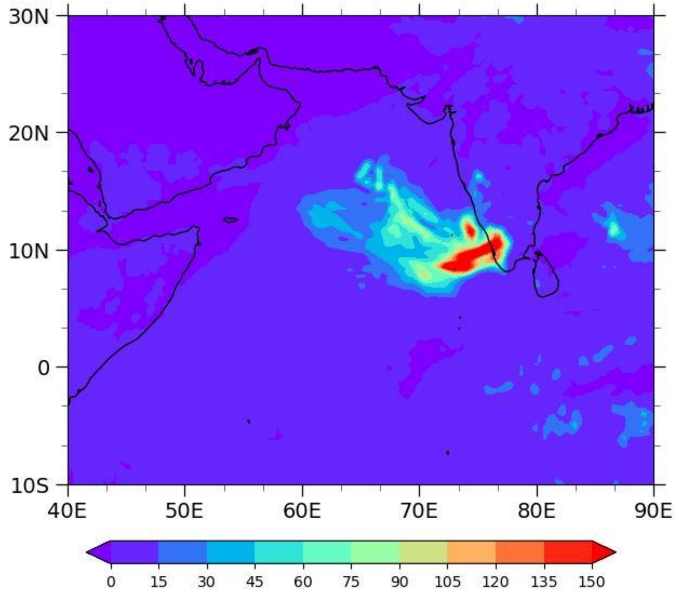

Total Precipitation: Initialized 2011-06-01T00 UTC, valid for 2011-06-01

P6

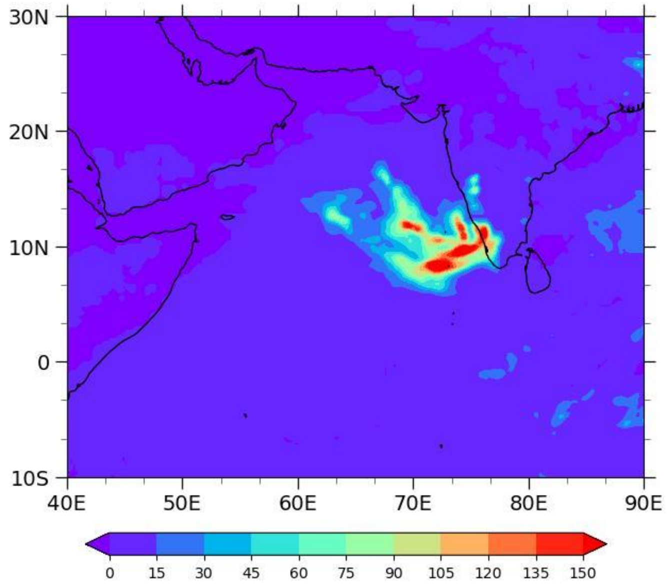

Total Precipitation: Initialized 2011-06-01T00 UTC, valid for 2011-06-01

P8

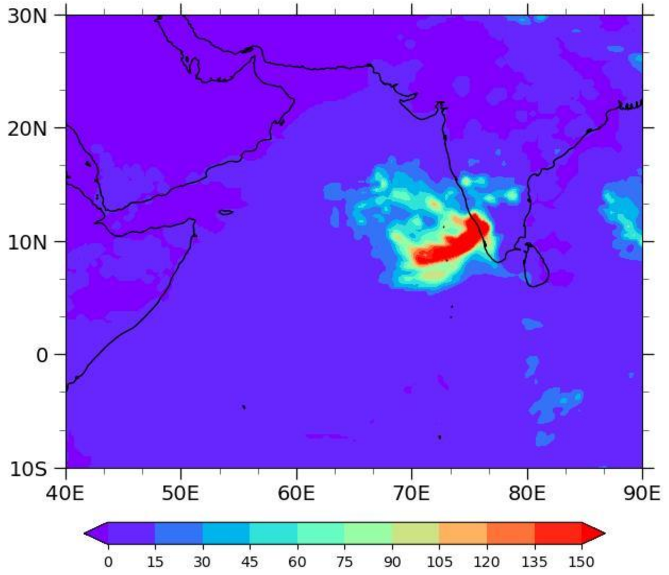

Daily Precipitation from GPM 20110601

GPM

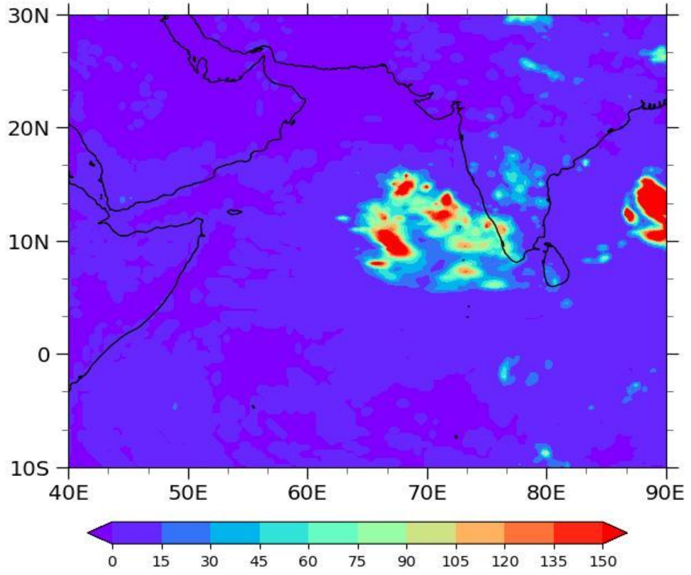

Some “UFS feature” causing the rainfall spatial pattern to remain very similar across the prototypes.

Initial Conditions

- Ocean: 3Dvar CPC
  Sea ice: CPC Ice analysis

- **For p5 and p6**:
  Atm and Soil: generated from CFSR
  Waves: generated with CFS forcings

- **For p8:**
  Atm, Waves: Same as p7 (Atm Generated from GEFS, waves generated with GEFS forcings)
  Soil and Snow: spin up of updated Noah-MP with NASA-GLDAS

A comparison of the UFS physics across the S2S prototypes

Reference: https://vlab.noaa.gov/web/ufs-r2o/dataproducts

Entity	P5 (GFSv15.2 Physics)	P6 (GFSv16 physics)	P8 (Candidate GFSv17 Physics)
Convection	Scale-aware Simplified Arakawa-Schubert Scheme	Same as P5	Convection updates
Boundary Layer	Hybrid Eddy-Diffusivity Mass-Flux (EDMF)	Replaced K-EDMF with sa-TKE-EDMF and revised background diffusivity as a stability dependent function; added a parameterization for subgrid scale nonstationary gravity-wave drag	Further PBL updates from P7 P7 had some parameterization updates and had Gravity wave drag parameterization (uGWD.v1 replacing uGWD.v0)
Radiation	RRTMG with Monte-Carlo Independent Column Approximation (McICA)	updated calculation of solar radiation absorption by water clouds, and updated cloud overlap assumptions	Radiation – updated calculation of solar radiation absorption by water clouds, and updated cloud overlap assumptions (from P6)
Microphysics	GFDL microphysics with 5 prognostics cloud species	updated GFDL microphysics scheme for computing ice cloud effective radius	Thompson microphysics
Land	Noah LSM	Noah LSM - revised ground heat flux calculation over snow covered surface, and introduced vegetation impact on surface energy budget over urban area; fractional grid for compositing fluxes on mixed land/water/ice cells	Noah-MP parameterization updates (for snow, land-atmosphere coupling, roughness length, sub-grid tiling) to correct P7 shortcomings
Atmosphere Levels	64	127	127
Ocean	GFDL MOM6, Hybrid-coordinates with tripolar grid, 0.25 degree global resolution. 75 hybrid levels, OM4 Set up [Adcroft, 2019]	Same as P5	Same as P5
Sea Ice	Los Alamos Sea Ice Model, version 6 (CICE6). Same grid as the ocean model. 5 thickness categories. No Mushy thermodynamics	Same as P5	Same as P5 but with Mushy thermodynamics turned on.
Waves	WAVEWATCH III wave model at 0.5 degree regular grid	Same as P5	Same as P5
Aerosols	-	-	GOCART (Chin et al., 2003) model at the atmospheric model resolution. Does not provide feedback to other components. Uses FENGSHA (Dong et al., 2016) dust scheme.